miRNA-26b Overexpression in Ulcerative Colitis-associated Carcinogenesis

Natalya Benderska, PhD,*,† Anna-Lena Dittrich, MS,*,† Sabine Knaup, MS,*,† Tilman T. Rau, MD,†
Clemens Neufert, MD, PhD,‡ Sven Wach, PhD,§ Fabian B. Fahlbusch, MD,‖ Manfred Rauh, PhD,‖
Ralph M. Wirtz, MD,¶ Abbas Agaimy, MD,† Swetha Srinivasan, MS,** Vijayalakshmi Mahadevan, PhD,**
Petra Rümmele, MD,†† Emmanouela Rapti, MD,‡‡ Maria Gazouli, MD, PhD,‡‡ Arndt Hartmann, MD, PhD,†
and Regine Schneider-Stock, PhD*,†

Background: Longstanding ulcerative colitis (UC) bears a high risk for development of UC-associated colorectal carcinoma (UCC). The inflammatory microenvironment influences microRNA expression, which in turn deregulates target gene expression. microRNA-26b (miR-26b) was shown to be instrumental in normal tissue growth and differentiation. Thus, we aimed to investigate the impact of miR-26b in inflammation-associated colorectal carcinogenesis.

Methods: Two different cohorts of patients were investigated. In the retrospective group, a tissue microarray with 38 samples from 17 UC/UCC patients was used for miR-26b in situ hybridization and quantitative reverse transcription polymerase chain reaction analyses. In the prospective group, we investigated miR-26b expression in 25 fresh–frozen colon biopsies and corresponding serum samples of 6 UC and 15 non-UC patients, respectively. In silico analysis, Ago2-RNA immunoprecipitation, luciferase reporter assay, quantitative reverse transcription polymerase chain reaction examination, and miR-26b mimic overexpression were employed for target validation.

Results: miR-26b expression was shown to be upregulated with disease progression in tissues and serum of UC and UCC patients. Using miR-26b and Ki-67 expression levels, an UCC was predicted with high accuracy. We identified 4 novel miR-26b targets (*DIP1, MDM2, CREBBP, BRCA1*). Among them, the downregulation of the E3 ubiquitin ligase DIP1 was closely related to death-associated protein kinase stabilization along the normal mucosa-UC-UCC sequence. In silico functional pathway analysis revealed that the common cellular pathways affected by miR-26b are highly related to cancerogenesis and the development of gastrointestinal diseases.

Conclusions: We suggest that miR-26b could serve as a biomarker for inflammation-associated processes in the gastrointestinal system. Because miR-26b expression is downregulated in sporadic colon cancer, it could discriminate between UCC and the sporadic cancer type.

(*Inflamm Bowel Dis* 2015;21:2039–2051)

Key Words: microRNA, miR-26b, inflammation, ulcerative colitis, colorectal carcinoma

Colorectal cancer (CRC) is one of the leading malignancies in Western Europe.[1] A subset of CRC is known to be etiopathologically linked with chronic inflammatory bowel disease (IBD), in particular to ulcerative colitis (UC). Statistically, 30% of patients with a long history of UC develop gastrointestinal cancer,[2] and UC is therefore considered a premalignant condition.[3] The pathogenesis

of UC-associated colorectal carcinoma (UCC) differs from the sporadic form and is characterized by distinct sequences and timing of genetic alterations. UCC demonstrates a "dysplasia-to-carcinoma" profile, whereas genetic hits in sporadic colon cancer follow an "adenoma-to-carcinoma" sequence.[4] Despite modern screening programs, about half of the patients with UCC are diagnosed at an already advanced tumor stage associated with a poor prognosis. Because of this diagnostic dilemma, novel biomarkers for early clinical risk assessment are needed.

MicroRNAs (miRNAs) are short 20 to 25 nucleotide RNA molecules that negatively regulate and fine-tune gene expression in eukaryotes by degradation of target messenger RNAs (mRNAs) or prevention of target mRNA transcription.[5,6] Up to 1000 miRNAs are expressed in human cells in a cell-specific and tissue-specific manner.[7] There is growing evidence that miRNAs have crucial function in specific cellular processes, such as differentiation, morphogenesis, proliferation, and apoptosis.[8–11] Recent studies have indicated that abnormal miRNA expression is a hallmark of cancer, suggesting that miRNAs may act as oncogenes or tumor suppressors.[8,10] Recently, it became evident that miRNAs are important players in inflammation.[7,12] For example, miR-146a and miR-146b are implicated in the nuclear factor kappa-light-chain-enhancer of activated B cells (NF-kB) pathway by downregulation of interleukin 1 receptor–associated kinase 1 and tumor necrosis factor (TNF) receptor–associated factor 6 protein levels.[13] Both miR-199a and miR-301a inhibit NF-kB–repressing factors and therefore elevate NF-kB activation in ovarian and pancreatic tumor cells, respectively.[14,15] Upregulation of miR-21 was found in IBD-associated dysplastic lesions.[16] Recently, 30 miRNAs with differential expression patterns in inflamed mucosa and inflammation-associated carcinoma tissues have been identified.[17] Interestingly, an miR-31 and miR-224 overexpression strongly mirrored the multistep tumor progression in IBD.[17,18] There were 3 miRNAs (miR-192, miR-375, and miR-422b), which were significantly decreased in active UC tissues, whereas 8 miRNAs (miR-16, miR-21, miR-23a, miR-24, miR-29a, miR-126, miR-195, and Let-7f) were significantly increased in active UC tissues, as compared with healthy control tissues.[19] So far, the impact of individual miRNAs during inflammation-associated carcinogenesis is not yet fully understood.

In our study, we focused on miRNA-26b (miR-26b), which is instrumental in normal tissue growth and development by its influence on cell proliferation and differentiation.[20] MiR-26b belongs to the family of hsa-miR-26 miRNAs together with miR-26a-1 and miR-26a-2. The sequence of the miR-26b seed region is highly evolutionarily conserved. The mature miR-26b sequence is similar to the sequence of miR-26a and differs only in 2 nucleotides. In some tumors, e.g., benign neoplasms of the pituitary,[21] gliomas,[22] and bladder cancers,[23] an upregulation of miR-26b has been observed compared with healthy tissue. In contrast, loss of miR-26b expression has been shown in breast cancer,[24] nasopharyngeal carcinomas,[25] and hepatocellular carcinomas.[26] Taken together, miR-26b acts as an oncomir or a tumor suppressor dependent on the cell type and experimental stimulus.

Interestingly, miR-26b serves as a tumor suppressor in sporadic colorectal carcinomas. Here an overexpression induces apoptosis in LoVo cell line and inhibits their invasive potential.[27] Similarly, miR-26b overexpression in SW480 colon tumor cells leads to inhibition of tumor growth because of a decrease of cell proliferation.[28]

So far, nearly nothing is known about the role of miR-26b in inflammation-associated colorectal carcinogenesis. Thus, the goal of our current study was to investigate the impact of miR-26b in UC-associated CRC.

We found that the expression of miR-26b was increased in human tissues from UC and UCC patients. Furthermore, we identified DIP1 as a novel target of miR-26b, which was confirmed by argonaute 2 (Ago2)-RNA immunoprecipitation (RIP), luciferase reporter assay, quantitative polymerase chain reaction (qPCR) examination, and immunohistochemical analysis. For the first time, we show evidence that miR-26b has the potential to be used as an inflammation-associated biomarker of the bowel in future.

MATERIALS AND METHODS

Human Specimen Collection

UC/UCC Samples

In this study, we used 2 different cohorts of patients. The diagnosis of IBD was based on standard clinical, endoscopic, radiological, and pathological criteria.[29] The first group (retrospective) was collected at the FAU Erlangen-Nürnberg, Germany, and the formalin-fixed and paraffin-embedded tissues were used in tissue microarray (TMA) format for In situ hybridization (ISH) and quantitative reverse transcription (qRT)-PCRs. The second group (prospective) included fresh–frozen biopsies and serum samples and was collected at the Gastroenterology Unit and the second Department of Surgery, "Aretaieio" Hospital, Athens, Greece, for qRT-PCRs.

TMAs in total contained 38 samples of 17 patients (7 female patients, 10 male patients, mean age 55 ± 25 years) diagnosed with UC or UCC. For each case, duplicates were punched, along with different controls, to ensure reproducibility and comparable stainings.

In the prospective group, we examined colon biopsies for 10 adult patients (6 female patients, 4 male patients, mean age 42.5 ± 14.5 years) with pathologically proven UC. Among these, 5 had pancolitis, 4 proctitis, and 1 proctosigmoiditis. Serum samples from these patients were examined, if available (n = 6). The healthy tissue cohort consisted of 15 patients (8 female patients, 7 male patients, mean age 41.6 ± 31 years), and the healthy blood group consisted of the same 15 patients, but only in 10 of them, we could detect target expression.

Crohn's Disease Samples

Fresh–frozen biopsies and blood samples were collected at the Gastroenterology Unit and the second Department of Surgery, Aretaieio Hospital, Athens (Greece). We examined colon biopsies

from 12 adult patients (7 female patients, 5 male patients, mean age 45.6 ± 14.5 years) with pathologically proven Crohn's disease (CD).

Celiac Disease Samples

Fasting serum samples of 14 healthy children (7 female patients, 7 male patients, mean age 7.6 ± 1.2 years) versus 15 age-matched pediatric patients with proven celiac disease[30,31] (10 female patients, 5 male patients, mean age 9.1 ± 0.9 years) were included in the analysis (collected December 2008–October 2011). These samples were a kind gift of the Department of Pediatric and Adolescent Health, FAU Erlangen-Nürnberg.

Experimental Model of Colon Carcinogenesis

Experimental model of inflammation-associated colorectal carcinogenesis was performed as previously described.[32] Briefly, 1× intraperitoneal injection of azoxymethane (AOM) (10 mg/kg) (Sigma-Aldrich, Taufkirchen, Germany) was followed by 3 cycles of dextran sulfate sodium (DSS) administration. Each cycle included 1 week of 2.5% (wt/vol) DSS (MP Biomedicals, Eschwege, Germany) in drinking water followed by 2 weeks of regular water. Serum was collected before treatment and at day 67. All experiments involving animals were performed according to the protocols approved by the Erlangen-Nürnberg University Animal Studies Committee.

Cell Culture

Human colorectal HCT116 tumor cells (mycoplasma free) were maintained in RPMI with 10% fetal bovine serum, supplemented with 1% penicillin–streptomycin. Cell line was authenticated using Multiplex Cell Authentication by Multiplexion (Heidelberg, Germany) as described previously.[33] Cells were cultured in either normal or TNF (Immunotools, Friesoythe, Germany, 0.66 ng/mL)-containing medium and incubated in a 5% CO_2 atmosphere at 37°C.

ISH for miRNA

ISH for miR-26b was performed on TMAs using the MiRCURY LNA miRNA ISH Optimization kit (Exiqon, Vedbaek, Denmark). Briefly, paraffin sections were deparaffinized and treated with 50 µg/mL proteinase K at 37°C for 20 minutes. After dehydration, slides were incubated with 50 nmol/L miR-26b locked nucleic acid probe (5′-DIG-ACCTATCCTGAATTACTTGAA-3′-DIG) at 52°C for 1 hour. This was followed by 5 individual stringency washes at hybridization temperature: twice with 5× saline sodium citrate, twice with 1× saline sodium citrate, and once with 0.2× saline sodium citrate buffers. Unspecific binding was blocked using the provided blocking solution (Exiqon) for 15 minutes. Alkaline phosphatase–conjugated anti-digoxigenin Fab fragments (diluted 1:500 in blocking reagent; Roche, Penzberg, Germany) were incubated at room temperature for 1 hour. After washing, enzymatic color development was performed by incubating the slides with 4-nitro-blue tetrazolium and 5-brom-4-chloro-3′-indolylphosphate substrate (NBT/BCIP substrate; Roche) at 30°C for 2 hours to allow formation of dark-blue 4-nitro-blue tetrazolium formazan precipitate, followed by nuclear fast red counterstain

(Vector Laboratories, Burlingame, CA) at room temperature for 10 minutes. Slides were subsequently dismantled in water, dehydrated in alcohol solutions, and mounted with mounting medium (Vector Laboratories). U6 small nuclear RNA–specific probe was used as system control (see Fig., Supplemental Digital Content 1, http://links.lww.com/IBD/A906). A standard 4-point scale method was used to evaluate the staining intensity under microscope, and the results were scored as follows: 0 (negative), 1 (+), 2 (++), or 3 (+++), according to the established criteria.[34]

RNA/miRNA Isolation and qRT-PCR

HCT116 Cells, Human Celiac Disease Serum, and Murine Serum

Total RNA, including miRNA, from HCT116 cells was prepared using the miRNeasy Mini kit (Qiagen, Hilden, Germany). The miRNeasy Serum/Plasma kit (Qiagen) was used for the preparation of miRNA from human and murine serum. RNA was converted into complementary DNAs (cDNA) with the miScript II RT kit (Qiagen). For the conversion of miRNA and mRNA, the 5× miScript HiFlex buffer was used. For the conversion of miRNA only, the 5× miScript HiSpec buffer was used. The experiment was conducted following the manufacturer's instructions. qPCR for miR-26b mature expression was done using miScript PCR System (Qiagen), including U6B as a reference gene. The cDNA was diluted stepwise to a 1 ng/µL concentration, and 2.5 µL were applied per reaction. Glyceraldehyde 3-phosphate dehydrogenase (GAPDH) served as a reference gene for normalization of target mRNA levels. The cycling profile for miRNA consisted of 95°C for 15 minutes followed by 40 cycles of denaturation at 95°C for 15 seconds, annealing at 60°C for 30 seconds, and elongation at 72°C for 30 seconds. The cycling profile for cDNA consisted of 95°C for 10 minutes followed by 40 cycles of denaturation at 95°C for 15 seconds and combined annealing/elongation step at 60°C for 1 minute. The QuantiTect SYBR Green PCR kit (Qiagen) was used. Samples were run in triplicate at least from 3 biological replicates. A non-template control was run in each experiment. Melting curve analyses were performed to confirm amplification specificity of the PCR products. PCRs were run on a C1000 Thermal Cycler CFX96 real-time PCR system (Bio-Rad, Hercules, CA). The obtained data were analyzed with the help of the CFX Manager software from Bio-Rad, and the $\Delta\Delta Ct$ values are reported.

FFPE Tissues

RNA from formalin-fixed paraffin-embedded TMA tissue was isolated commercially (Stratifyer Molecular Pathology GmbH, Cologne, Germany). RNA was extracted using germanium-coated magnetic beads (XTRAKT kit; Stratifyer Molecular Pathology GmbH). The method involves extraction-integrated deparaffinization and DNase I digestion steps. The quality and quantity of RNA were checked by measuring CALM2 expression as a surrogate for amplifiable mRNA by qRT-PCR. CALM2 was used as endogenous reference. For the determination of MKI-67 and CALM2 mRNA levels, PCR Primers and 5′-FAM–3′-TAMRA–labeled hydrolysis

probes were selected using Primer Express software, Version 2.2 and 3 (Applied Biosystems/Life Technologies, Karlsruhe, Germany). Primers and probes were purchased from Eurogentec S.A. (Seraing, Belgium). For qPCR, 0.5 μM of each primer and 0.25 μM of each probe were used. All qRT-PCRs were performed in triplicates using the SuperScript III Platinum One-Step qRT-PCR kit with ROX (Invitrogen/Life Technologies, Darmstadt, Germany) according to the manufacturer's instructions. Experiments were performed on a Stratagene Mx3005p (Agilent Technologies, Böblingen, Germany) with 30 minutes at 50°C and 2 minutes at 95°C followed by 40 cycles of 15 seconds at 95°C and 30 seconds at 60°C. Relative expression levels were calculated using the ΔΔCt method. A commercially available human reference RNA (Stratagene qPCR Human Reference Total RNA; Agilent Technologies) was used as positive control. Non-template controls were assessed in parallel to exclude contamination.

Human Fresh–Frozen Colon Biopsies and Human Serum

miRNAs from tissues and serum samples were purified using the mirVANA miRNA isolation kit (Applied Biosystems, Foster City, CA) according to the manufacturer's instruction. The expression patterns of miR-26b tested and a housekeeping gene U6B were quantitatively assayed using reverse transcription and qRT-PCR. Stem loop cDNAs were synthesized using looped reverse transcription primer specific for each miRNA. All the materials were purchased from Exiqon. All samples were analyzed twice to confirm reproducibility. Real-time PCRs were conducted on an ABI Prism 7700 apparatus (Applied Biosystems). The expression of miR-26b was normalized to U6B RNA internal control. The relative level of miRNA expression was calculated using the ΔΔCt method.

Primers were purchased from Metabion GmbH (Planegg, Germany), and miRNA Primer assays were obtained from (Qiagen). Their sequences are presented in the Table, Supplemental Digital Content 2, http://links.lww.com/IBD/A907.

Luciferase Reporter Assays

Luciferase reporter vectors containing the 3-UTR of miR-26b target gene DIP1 were generated after PCR amplification from human cDNA and cloned into the pmirGLO Dual-Luciferase miRNA Target Expression Vector (Promega, Madison, WI), immediately downstream from the stop codon of the luciferase gene. The sequence of each insert was confirmed by sequencing. MiR-26b was obtained by annealing, purifying, and cloning short oligonucleotides containing the perfect miRNA-binding site into the NheI and AccI sites of the pmirGLO Vector. HCT116 cells were plated in 24-well plates and 24 hours later cotransfected with 50 ng of the pmirGLO dual-luciferase constructs, containing the indicated 3′-UTRs of target gene, and with 32 nM pre-miR miRNA Precursor Molecules-Negative Control or pre-miR miRNA Precursor hsa-miR-26b (PM10939) using Lipofectamine 2000 (Invitrogen/Life Technologies). Lysates were collected 24 hours after transfection, and Firefly and Renilla Luciferase activities were

consecutively measured using Dual-Luciferase Reporter Assay (Promega) according to the manufacturer's instructions. Relative luciferase activity was calculated by normalizing the ratio of Firefly/Renilla luciferase to that of negative control–transfected cells. Transfections were performed in triplicate and repeated 3 to 4 times.

Argonaute2 RNA Immunoprecipitation

We used an Ago2 monoclonal antibody for immunoprecipitation (IP) to identify the miRNA-mediated recruitment of different transcripts to the RNA-induced silencing complex.[35] The experiment was done according to the EZ-Magna RIP instruction (Cat. No.17-701; Merck Millipore, Darmstadt, Germany). Briefly, 10^6 cells were seeded in 150-mm dishes and transfected with 1200 pmol of negative control or the hsa-miR-26b mimic (Ambion, Darmstadt, Germany). For the transfection of miRNA mimics into HCT116, the Lipofectamine 2000 (Invitrogen) was used. The cell pellet was collected 24 hours after the transfection, dissolved in 200 μL lysis buffer, and incubated with 5 μg of anti-Ago2 (RIPab+ Ago2 clone 9E8.2; Merck Millipore) or rabbit anti-IgG (IGG, GT X RT; Merck Millipore) antibodies bound to magnetic beads overnight. After IP, sample aliquots were subjected to Western blot analysis for verification of Ago2 binding. The rest of the samples were incubated with protein kinase K at 55°C for 30 minutes for protein digestion. RNA was purified using phenol/chloroform extraction according to the manufacturer's protocol (Merck Millipore).

Overexpression of miRNA

Expression of miR-26a/b in HCT116 cells was increased by transfection with miR-26a/b mimics (Ambion). The cells were plated in 24-well plates for 24 hours and then transfected using Lipofectamine 2000 (Invitrogen). The transfection medium was changed after 6 hours, and the cells were supplied with fresh TNF-containing medium. Cells were harvested at 24 to 48 hours after TNF stimulus.

Western Blot Assay

Cells were lysed with urea lysis buffer. Protein concentration was determined by Bio-Rad Dc Protein Assay (Bio-Rad). Equal amount of cell lysate (30 μg) was resolved on sodium dodecyl sulfate polyacrylamide gel electrophoresis and analyzed by Western blot. Antibodies used in this study were as follows: rabbit monoclonal DIP1 (Abcam, Cambridge, United Kingdom), death-associated protein kinase (DAPK) mouse monoclonal (BD Biosciences, San Diego, CA), mouse monoclonal MDM2 (Merck Millipore), and GAPDH horseradish peroxidase linked (Abnova, Heidelberg, Germany). ImageJ software (v.1.45s) was used for quantification of band intensities.

Target Prediction for miR-26b, Which Overlaps with DAPK

For qPCR analysis, a preselection of potential miR-26b target genes and DAPK interaction partners has been performed. The miR-26b targets were predicted in silico from 7 prediction programs (DIANA-mT, miRanda, miRDB, miRWalk, TargetScan, miRecords and Tarbase). The identified targets were compared with the DAPK

interaction partners as listed by BioGRID and String 9.05 databases. Only miRNA targets that were predicted by a minimum of 4 different programs were considered for further analysis (Fig. 4A).

Ingenuity Pathway Analysis Functional Pathway Analysis

For further pathway analysis of biological and molecular networks underlying UC, we used the web-based Ingenuity Pathway Analysis tool (IPA; Ingenuity Systems, Redwood City, CA; www.ingenuity.com), as described in detail earlier.[36] Using IPA, we were able to compare our filtered microarray data (Fig. 4A) with the current Ingenuity Pathway Knowledge Base (as of October 10, 2014). Based on our list of significantly altered miR-26b target genes and DAPK interaction partners (Fig. 4A), IPA computed sets for the comparative analysis of generic networks (i.e., inflammation, proliferation, and apoptosis). No fold change cutoff was applied to the normalized output data ($P < 0.05$). Comparative network analysis was carried out using the web-based software BioVenn by Hulsen et al.[37] For functional pathway analysis, the confidence level was set to "experimentally observed," including direct and indirect relationships, with cutoff settings of 2.0-fold (up and down) and P value <0.05. Mammal (human, mouse, and rat) orthologs of each gene were included in the analysis.

Statistical Analyses

Results are expressed as mean ± SD or mean ± SEM when independent experiments were performed in replicates. Cluster analysis by Ward's minimum variance method was performed by JMP 9.0.0 software package (SAS Institute Inc.; Cary, NC). We used Mann–Whitney U test or Student's *t* test (GraphPad Prism software; GraphPad, San Diego) for different comparisons where appropriate. P values <0.05 were considered significant.

Ethical Consideration

Before the commencement of the study, the ethics committee at the participating hospitals had approved the recruitment protocols. For the prospective study, an informed consent was obtained from all the participants.

RESULTS

MiR-26b Staining Intensity Increases in UC and UCC

MiR-26b ISH was performed on a TMA of 38 samples from 17 patients. ISH signal was seen in all cases with variation in staining intensity. In addition to epithelial tumor cells, positive staining was also observed in some cells of the lamina propria, e.g., stromal cells and lymphocytes. In the UCC, this slight background activity is maintained in the surrounding microenvironment; however, the epithelial positivity is dominant in both UC and UCC cases. Using a semiquantitative approach, we gradually scored the miR-26b tumor epithelial staining[1–3] as described in the Materials and Methods. The miR-26b ISH signal significantly increased from the control group with inactive UC to the active UC group and from the active UC to the UCC group (Fig. 1A–F, G). This gradual increase was also observed when comparing areas with different stages of individual patients (Fig. 1H). We found a significant correlation between the miR-26b expression and the histopathological status of the tissue (R = 0.824, $P < 0.0001$).

In addition, we isolated RNA from TMA-derived samples, and the expression of proliferation marker gene MKI-67 (Ki-67) was assessed by qRT-PCR (Fig. 1I). We also found a significant correlation between the expression of Ki-67 and miR-26b ISH (R = 0.43, $P < 0.0064$). Two-dimensional hierarchic clustering of quantitative miR-26b and MKI-67 RNA data revealed 4 different groups (Fig. 1I). These groups showed (1) high expression of miR-26b and high or moderate Ki-67 expression (orange color), (2) moderate expression of Ki-67 and no expression of miR-26b (blue color), and (3) low expression of miR-26b but high Ki-67 levels (green color), and (4) a larger dominant group showed low expression for both markers (red color). Interestingly, the clustering was highly associated with the histological subtype. Particularly, the carcinoma-enriched cluster contained 93% of all carcinoma samples, suggesting a potential for miR-26b as a biomarker in the diagnosis of UC and UCC (Fig. 1I). In contrast, inactive colitis had very low RNA levels of both markers, whereas active colitis had elevated levels of either MKI-67 or miR-26b.

MiR-26b Expression Increases in Human Biopsies and Serum of Patients with IBD

The expression level of miR-26b was investigated by qRT-PCR in fresh–frozen colon biopsies from UC patients. A significant elevation of miR-26b expression in UC biopsies was found compared with the healthy control group (Fig. 2A). Next, we examined miR-26b expression in the blood serum of UC patients because levels of circulating miRNAs can be altered in several clinical diseases and may hence serve as potential biomarkers.[38] Indeed, similar to our tissue-derived data, miR-26b was significantly upregulated in patients with UC compared with the healthy donor group (Fig. 2B).

To investigate whether miR-26b expression was altered in other inflammation-associated disorders of the gut system, we examined further blood serum from 2 groups: (1) a group of adult patients with CD and (2) a pediatric group of patients with celiac disease. In both patient cohorts, our data demonstrated a significant upregulation of miR-26b expression compared with the respective healthy control group (Fig., Supplemental Digital Content 3, http://links.lww.com/IBD/A908; Fig. 2A, B, C). These results underline an important role of miR-26b in the inflammation processes of the gastrointestinal tract.

Expression of miR-26b in AOM/DSS Colon Cancer Model

We expanded our study on chemically induced murine model of CRC. Mice were treated with AOM/DSS, which causes inflammation-associated tumor formation in the colon (Fig. 3A). We investigated the expression of circulating miR-26b in murine
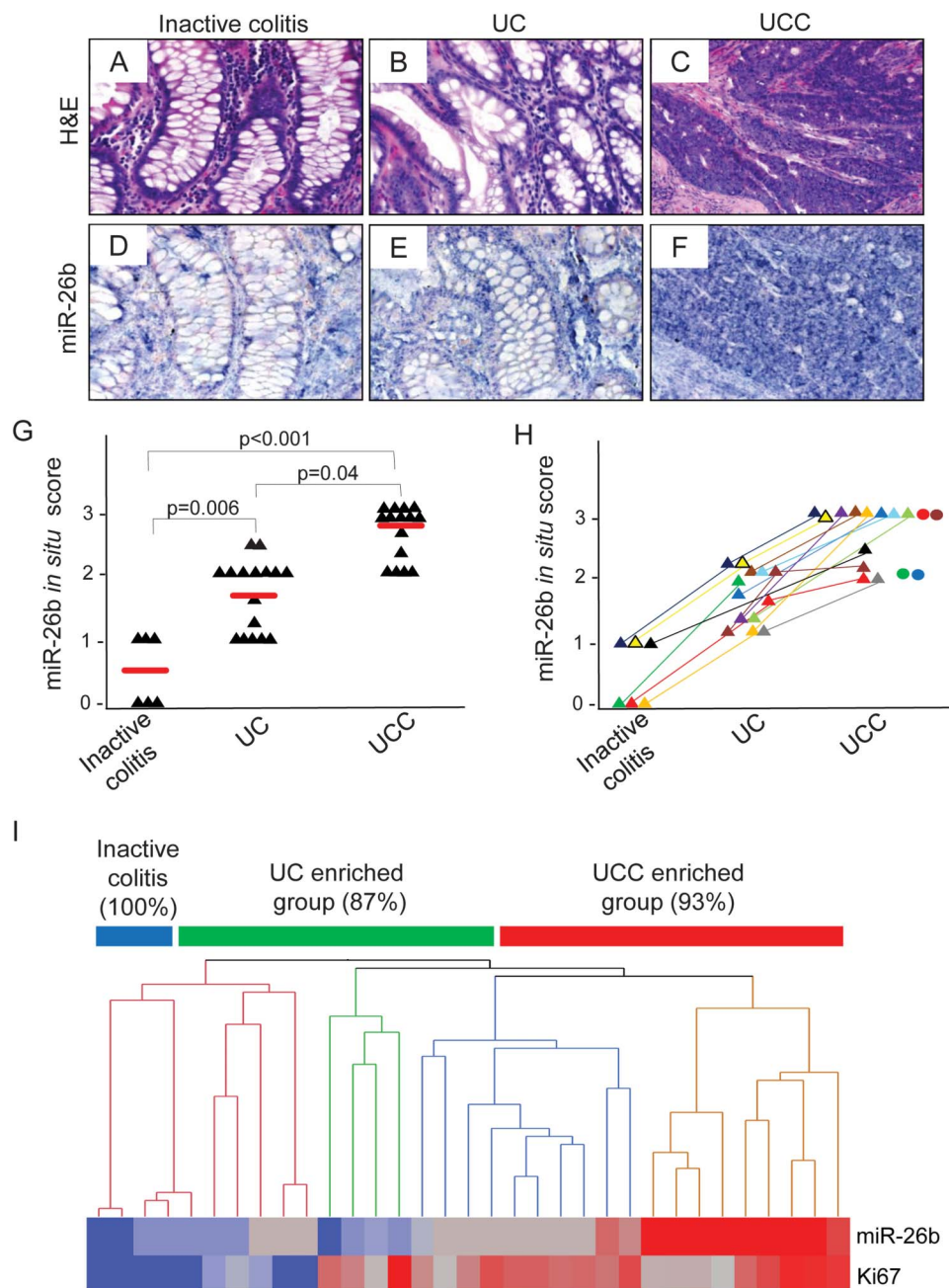
FIGURE 1. miR-26b expression in human UC and UC-associated carcinomas (UCC) determined by ISH. A, Hematoxylin and eosin (H&E) staining (top panel) and ISH (bottom panel) for miR-26b expression in inactive colitis (A, D), active UC (B, E), and UCC (C, F) at ×40 magnification. G, ISH scores (0–3) of miR-26b from 38 samples of 17 patients, as described in Materials and Methods, presented as the average scores of 2 independent observers (T.T.R. and A.A.). Samples were grouped according to their pathological stage: inactive colitis (n = 6), active UC (n = 16), and UCC (n = 16). H, Individual ISH scores (0–3) of miR-26b, as described in Materials and Methods. Data are presented as average score. Tissue samples were grouped according to their pathological disease status within a single patient. Nine patients had available samples in an "inactive colitis-UCC" sequence, 4 patients had "UC-UCC" sequence, and 1 patient had "inactive-UC" sequence. Four patients having only UCC samples were indicated as a circle. I, Graphical representation of 2-dimensional hierarchical clustering results on miR-26b ISH data and mRNA qPCR profiles of Ki-67 of inactive colitis (n = 6), active UC (n = 16), and UCC (n = 16) samples. RNA expression scores are depicted according to a color scale: red, positive expression; blue, negative expression; and gray, intermediate expression. Dendrogram of samples discriminates between the 4 groups (indicated in purple, green, blue, and orange).
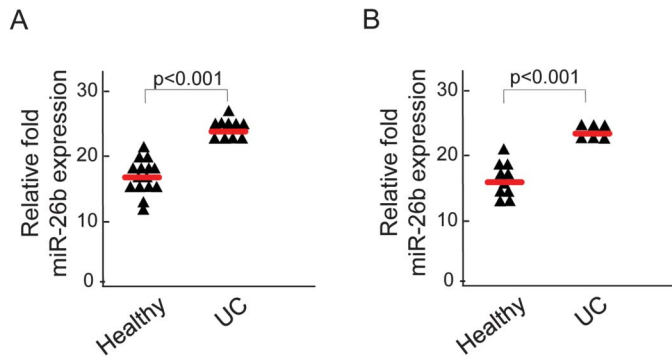
A

B

FIGURE 2. miR-26b expression in human UC determined by quantitative PCR. A, Individual relative expression of miR-26b in healthy people with normal uninflamed colon mucosa (n = 15) and patients with active UC (n = 10) in biopsy specimens determined by qRT-PCR. Analyses were performed in triplicates, and the results were normalized using the U6 expression level; $P < 0.0001$ (unpaired 2-tailed t test). B, Individual relative expression of miR-26b determined by qRT-PCR in healthy people (n = 10) and patients with active UC (n = 6) in blood serum. In 5 healthy samples, miR-26b/U6 was not amplifiable. Analyses were performed in triplicates, and the results were normalized using the U6 expression level, $P < 0.0001$ (unpaired 2-tailed t test).

serum obtained before and after applying the AOM/DSS protocol. Quantitative PCR analysis indicated an increase in the miR-26b expression level in serum of mice carrying colon tumors compared with the untreated controls, suggesting that miR-26b upregulation might be associated with tumor progression in this model (Fig. 3B).

MiR-26b Is Connected with DAPK Interaction Partners

It was shown that the majority of potential cancer-associated targets regulated by the miR-26 family belongs to

the class of protein kinases.[39] Our previous studies defined an increase of DAPK protein expression paralleling UC-associated carcinogenesis.[40] Therefore, we aimed to identify proteins that are connected with DAPK through miR-26b. Analysis of public databases revealed 7 genes, which were predicted as DAPK interaction partners and were simultaneously found to be potentially regulated by miR-26b (Fig. 4A, B). To validate these proteins as potential miR-26b targets, we performed an RIP assay in an in vivo cellular context. The results showed that DIP1, MDM2, BRCA1, PTEN, and CREBBP were significantly enriched in the Ago2-immunoprecipitated RNAs of the HCT116 cells transfected with miR-26b mimic compared with those cells treated with scrambled miRNA only (Fig. 4C). The levels of TSC1 and ATM enrichment in miR-26b precipitants were insufficiently comparative with the scrambled precipitants, and therefore, they were not validated as targets for miR-26b (Fig. 4C). Because PTEN was already experimentally shown as an miR-26b target,[21] we excluded it from further studies. Interestingly, we found that two DAPK interaction partners targeted by miR-26b, i.e., DIP1 and MDM2, belong to E3 ubiquitin–protein ligases and are associated with protein stabilization processes. DIP1 is well known to regulate DAPK directly by inducing its proteosomal degradation.[41] In contrast to DIP1, the MDM2 "ubiquitination signal" blocks the interaction between DAPK and p53, subsequently diminishing DAPK signaling.[42]

To verify the decrease of MDM2 and DIP1 protein expression under inflammation, we performed Western blot analysis after TNF treatment of HCT116 cells. We found that DIP1 protein expression was notably diminished in tumor cells in a time-dependent manner (Fig. 4D), whereas MDM2 protein level was upregulated at 1 and 6 hours but decreased only at later time points. This suggests the involvement of alternative
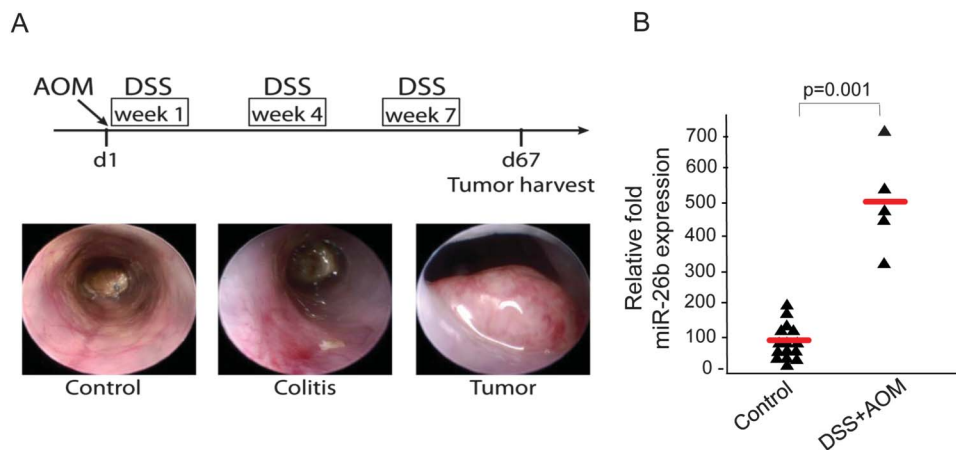
A

B

FIGURE 3. Expression of miR-26b in AOM/DSS-induced murine model of CRC. A, Upper panel: scheme of 4-stage protocol inducing chronic inflammation and colitis-driven tumors in mice. Lower panel: endoscopic images display the development of tumors in the murine colon after AOM/DSS treatment. B, Individual relative expression of miR-26b in murine serum of control (day 1, n = 15) and AOM + DSS–treated mice (day 67, n = 5) measured by qRT-PCR. Analyses were performed in triplicates, and the results were normalized using the U6 expression level. $P = 0.0001$ compared with untreated samples (Mann–Whitney U test).
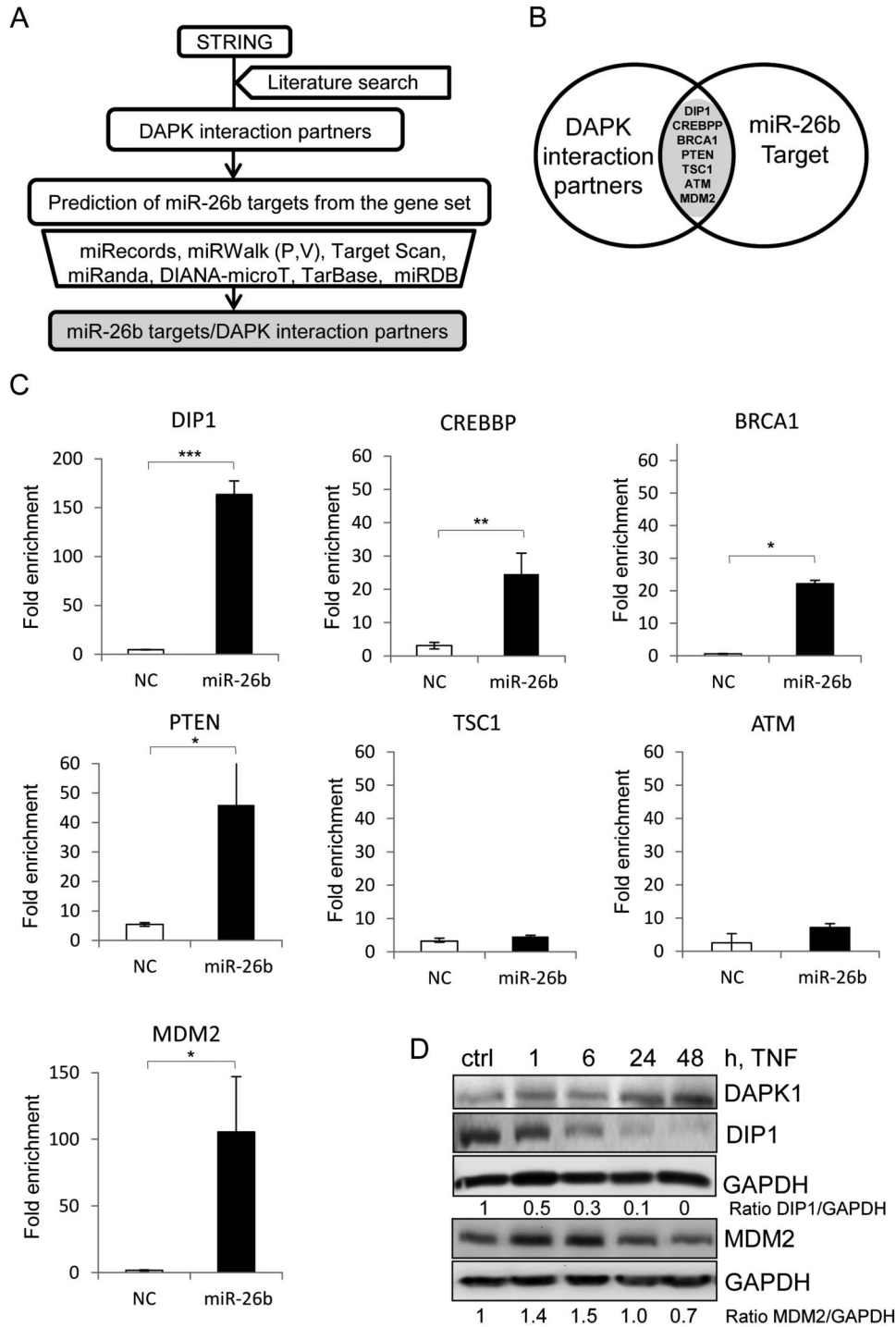
FIGURE 4. MiR-26b targets associated with DAPK. A, Schematic representation of the strategy used to reveal DAPK-interacting proteins connected through miR-26b. B, Venn diagram illustrating candidates overlapping between miR-26b–specific targets and DAPK-interacting partners. C, Relative enrichment of miR-26b targets identified by Ago2-RIP in HCT116 cells. Expression signals of Ago2-bound RNA were normalized to the IgG-bound RNA from the same cell population, and enrichments of miR-26b–transfected versus scrambled miR–transfected cells (negative control [NC]) were calculated using ΔCt method. Ago2-RIP was repeated twice and qRT-PCR performed 3 times in triplicates. Results are expressed as mean $\pm$ SD. $*P < 0.05$; $**P < 0.01$; $***P < 0.001$ compared with scrambled transfection (unpaired 2-tailed t test). D, Western blot analysis of HCT116 cells treated with TNF (0.66 ng/mL). At the indicated time points, whole-cell lysates were prepared and equal amounts of proteins were resolved by sodium dodecyl sulfate polyacrylamide gel electrophoresis and probed with specific indicated antibodies. Anti-GAPDH antibody was used as a loading control. Experiments were repeated 3 times, and representative images are shown.

TNF-mediated regulatory mechanisms for MDM2 in HCT116 cells (Fig. 4D). As known from previous studies,[40,43] the DAPK protein level was enhanced during the TNF treatment. Based on these data, we decided to investigate the miR-26b/DIP1/DAPK axis in more detail.

MiR-26b Regulates DIP1 Expression

In addition to Ago2-IP, which demonstrated a strong enrichment for DIP1 among other targets (approximately 160-fold, Fig. 4C), we employed a luciferase reporter assay to investigate whether miR-26b directly binds to DIP1 mRNA. We identified a putative miR-26b–binding site at positions 4046 to 4052 in the 3′-UTR of DIP1 mRNA using TargetScan algorithms (Fig. 5A). Next, we cloned the predicted miR-26b–binding site from DIP1 mRNA into a luciferase reporter vector and cotransfected the cloned plasmid with either scrambled miRNA or miR-26b into HCT116 cells. MiR-26b significantly inhibited the luciferase activity compared with the scrambled miRNA (Fig. 5B). In addition, miR-26b did not suppress the luciferase activity of the reporter vector containing 3′-UTR of DIP1 with single-point mutations in the miR-26b–binding site (Fig. 5B). These results suggested that miR-26b directly interacts with the 3′-UTR of DIP1 mRNA. In agreement with our

data, overexpression with miR-26a and miR-26b mimics showed a downregulation of DIP1 and an upregulation of DAPK only with miR-26b, indicating a higher specificity of miR-26b to target DIP1. This effect was enforced by TNF application (Fig. 5C).

Finally, to verify our hypothesis in vivo, we tested DIP1 mRNA expression level in tissue biopsies of UC patients by qRT-PCR. Indeed, DIP1 mRNA was downregulated in samples of UC in biopsies (Fig. 5E).

Altogether, these data show that miR-26b directly targets DIP1, which in turn leads to the upregulation of cellular DAPK protein level. This mechanism was already demonstrated to play an important role in inflammation-associated tumor transformation.[40]

Pathway Analysis for miR-26b Target Genes

The miRNA-target regulation network was analyzed in more detail using in silico functional pathway analysis (IPA). IPA pathway algorithm showed that miR-26b target genes play a critical role in cellular oxidative stress (Fig. 6A), which is known to have a significant impact during tumorigenesis. Therefore, it is not surprising that the networks of cancer and gastrointestinal diseases received the highest IPA ranking along with other biofunctions associated with miR-26b regulation (Fig. 6B). Most of the predicted
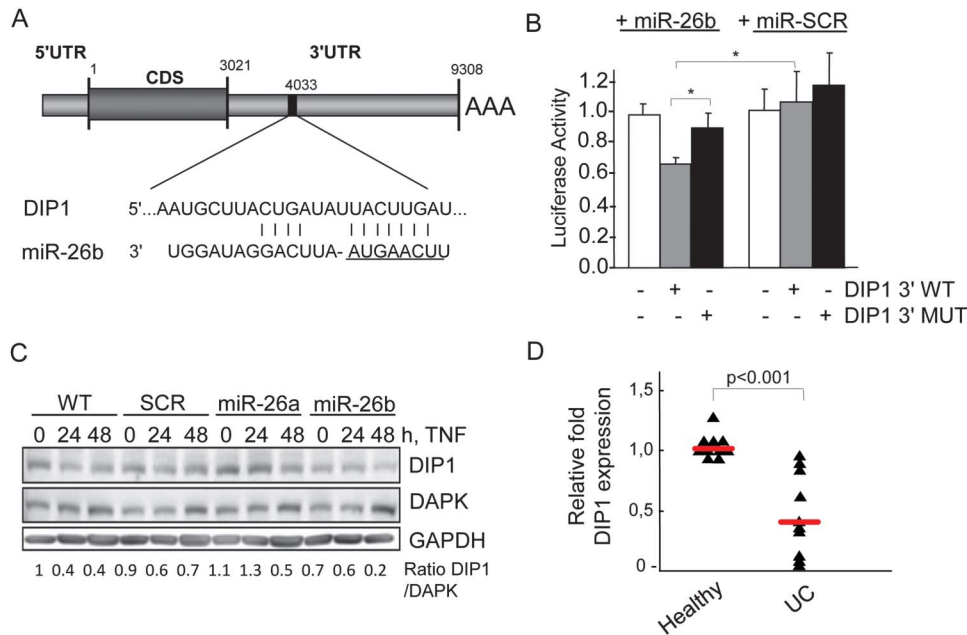

FIGURE 5. MiR-26b targets DIP1 in vitro and in vivo. A, miR-26b sequences in the 3′-UTR of human DIP1 mRNA as predicted by TargetScan (v.5.1). The miR-26b seed sequence and its predicted binding site in the DIP1 3′-UTR are shown underlined. B, HCT116 cells were cotransfected with the vectors containing the full-length 3′-UTR, mutated 3′-UTR, or an empty pmirGLO vector (250 ng/mL) and an miR-26b mimic (20 nM) or miR scramble (20 nM). Firefly luciferase activity was measured 24 hours later and normalized to Renilla luciferase activity. The experiment was done 3 times in triplicates. Results are expressed as mean ± SD. *P < 0.05 (unpaired 2-tailed *t* test). C, HCT116 cells were transfected with 20 nM miRNA mimics for 6 hours and then treated with TNF (0.66 ng/mL) for indicated time points. The protein expression was assayed by Western blot using indicated antibodies. Anti-GAPDH antibody was used as a loading control. Band densities were quantified using ImageJ. Experiments were repeated 3 times, and representative images are shown. D, Relative expression of DIP1 mRNA was determined by qRT-PCR from biopsy specimens of healthy cohort (n = 10) and patients with active UC (n = 10). In 5 healthy samples, DIP1 mRNA was not amplifiable. Results were normalized using GAPDH expression level and performed at least 3 times in triplicates.
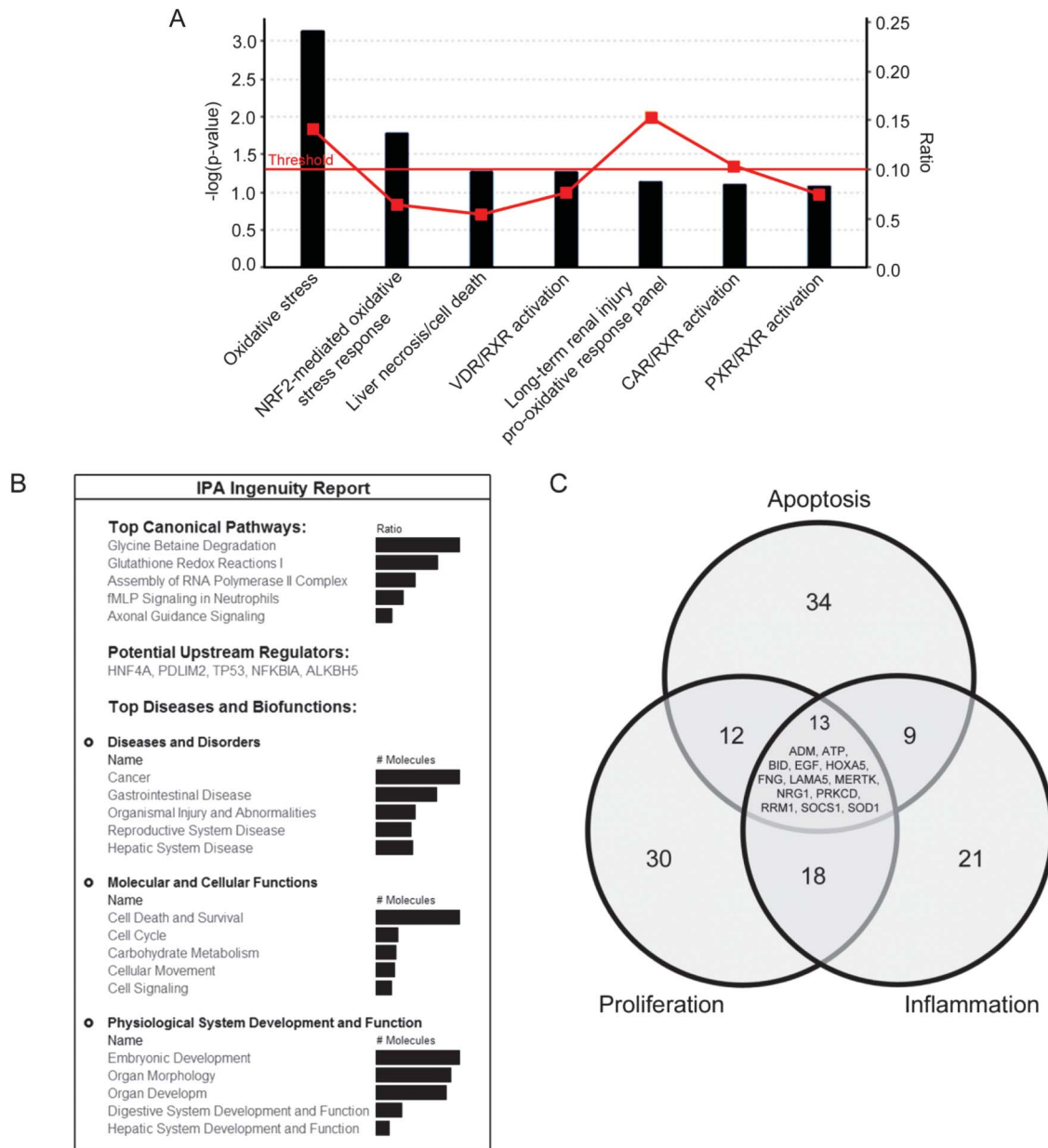
FIGURE 6. IPA-assisted network analysis of miR-26b target genes/DAPK interaction partners. A, IPA toxicology report. B, IPA: canonical pathways, diseases, and biofunctions. C, Comparative pathway analysis: overlay of potential target genes involved in apoptosis, proliferation, and inflammation.

miR-26 targets were found to be involved in different pathways of cell metabolism, such as glycine–betaine degradation, glutathione redox reactions, and assembly of RNA polymerase II complex. Through their contribution to cell function, the majority of miR-26b–mediated targets belong to the "cell death and survival" group. Comparative analysis of the genetic networks of inflammation, proliferation, and apoptosis led to the identification of a subgroup of 13 miR-26b targets (APM, ATP, BID, EGF, HOXA5, IFNγ, LAMA5, MERTK, NRG1, PRKCD, RRM1, SOCS1, and SOD1) (Fig. 6C). This could suggest that miR-26b might mediate cross talk of divergent pathways by regulating single genes.

DISCUSSION

Chronic inflammation alters the expression of genes, including protein-coding and noncoding miRNA genes, subsequently predisposing cells for neoplastic transformation. MiRNA dysregulation influences multiple biological processes related to cancerogenesis, including cell proliferation and apoptosis. Moreover, it can trigger proinflammatory and anti-inflammatory cellular responses.[44]

Recently, miR-26 has been shown to be associated with inflammation.[45,46] Although downregulation of miR-26b appears to represent a common event in sporadic colorectal carcinogenesis, so

far no studies have directly addressed the role of miR-26b in inflammation-associated colorectal carcinogenesis.

We analyzed the miR-26b expression profiles in patients with inactive and active UC and UCC. The fact that our study was performed independently on 2 cohorts of patient's specimen collected at Erlangen University (Germany) and Athens Medical School (Greece) strengthens our findings. For the first time, we demonstrated that miR-26b was significantly overexpressed in both human tissues and serum of patients with active UC, in tissues of patients with UCC, and TNF-treated colorectal HCT116 tumor cells. We also found that miR-26b expression was significantly upregulated in an experimental mouse model of chemically induced colitis, suggesting its role in tumor transformation. We demonstrated that miR-26b directly targets the E3-ligase DIP1 in human CRC cells and downregulates its expression. This may activate signaling pathways of DIP1 substrates, in particular DAPK-mediated cascades.

Our previous studies indicated that DAPK plays an important role in balancing inflammatory conditions along UC-associated carcinogenesis showing a gradual upregulation along severity of the disease.[40] TNF induces both proinflammatory interleukin 6/STAT3 and anti-inflammatory DAPK signaling. Activated STAT3 represses DAPK expression at the transcription level, whereas DAPK inhibits pSTAT3^{Y705} phosphorylation and secretion of interleukin 6 upon stimulation by TNF. Because recent transcriptional and posttranscriptional DAPK regulatory mechanisms are under intensive investigations,[47] we were interested in examining whether potential targets of miR-26b could influence DAPK function. In our study, we experimentally validated DIP1, CREBBP, BRCA1, and MDM2 as new miR-26b targets in colorectal tumor cells by Ago2-RIP. To our knowledge, the functional connections between DAPK and BRCA1, and DAPK and CREBBP have not yet been reported in the literature. We focused on DIP1 and MDM2 because their significance for the DAPK function has been already shown.[41,42,48–50] Interestingly, both candidates possess E3 ubiquitin ligase activity and are engaged in the regulation of cellular protein turnover. Because MDM2 protein expression increased at early time points after TNF treatment and is decreased only at later time points, we suggest alternative TNF-mediated regulatory mechanism for MDM2. Thus, we focused on our mechanistic studies on DIP1. Ago2-RNA IP and luciferase reporter assay indicated that miR-26b directly targets DIP1 3′-UTR through the predicted binding site at positions 4046 to 4052.

DIP1 is a multidomain E3 ubiquitin ligase with 3 carboxyl-terminal RING finger domains. It was shown to target the Notch ligands Delta and Jagged as part of activation of the Notch signaling pathway.[51–53] In addition, DIP1 is involved in the regulation of apoptosis: (1) by decreasing the association of caspase-8 and cFLIP[54] and (2) by depletion of the stability and cellular levels of DAPK.[48] Indeed, TNF-induced upregulation of miR-26b in HCT116 colon cancer cells inhibited DIP1 expression and stabilized the DAPK protein. Furthermore, we verified the clinical relevance of the miR-26b/DIP1/DAPK axis in colon biopsies of UC patients by showing an inverse correlation between miR-26b and DIP gene expressions.

In the last years, several miRNA profiling studies based on the tissue or blood samples from patients with IBD were performed to improve diagnostics and possible treatment of this disease. In one of them, the authors found an UC-associated increase of miR-26b expression, however, without a statistical significance.[55] We found that the expression of miR-26b gradually increases during progression from inactive colitis to active colitis with the highest level in cancer. Of note, a statistically significant increase in miR-26b expression was observed at both UC and UCC groups in comparison with inactive colitis. Two-way hierarchical clustering could distinguish patients in the UCC and non-UCC groups based on the expression profiling of Ki-67 and miR-26b with a high accuracy of 93%. This suggested that miR-26b expression level may be a useful clinical marker for predicting UC-associated neoplasms. However, future studies involving higher number of patients are required in this context.

Recently, circulating miRNAs in the serum were found to show specific expression patterns, reflecting physiological and pathological processes.[56,57] Because it was shown that serum miRNAs are more resistant to ribonuclease activity, changes of temperature, extreme pH, long storage, or freeze-thaw steps,[58,59] circulating miRNAs are considered as promising biomarkers for disease diagnostics.[38] In addition to identification of miR-26b expression in tissue biopsies of patients with UC, we evaluated its level in blood serum from the same patients. Interestingly, the data obtained from human tissues and corresponding serum samples show nearly analogous values, suggesting potential application of miR-26b determination in clinical diagnostics by noninvasive methods. It would be interesting to investigate the correlation of miR-26b with patient's clinicopathological data, which is impossible at the moment because of limited number of samples.

The miR-26b–associated network was further evaluated using an integration pathway analysis. Interestingly, miR-26b targets were mainly conjugated to gastrointestinal pathologies. Indeed, we found a significant increase of miR-26b in CD and celiac disease, 2 other types of gastrointestinal inflammation-associated disorders, underscoring the involvement of miR-26b in gut inflammation. Consistent with our findings, Bai et al[60] showed that miR-26b together with miR-146a, -335, and -124 demonstrated the greatest influence (>70%) on the risk genes, common for UC, CD, and CRC diseases.

In summary, we present new insights into the inflammation-associated regulatory network of miR-26b. We suggest that (1) miR-26b can discriminate between sporadic and UC-associated carcinomas and between different stages of UC-associated carcinogenesis, (2) miR-26b is a potential biomarker for inflammation-associated processes in the gastrointestinal system, and (3) there is an important role of the miR-26b/DIP1/DAPK axis in inflammation.

REFERENCES

1. Ferlay J, Steliarova-Foucher E, Lortet-Tieulent J, et al. Cancer incidence and mortality patterns in Europe: estimates for 40 countries in 2012. *Eur J Cancer.* 2013;49:1374–1403.

2. Bernstein CN, Blanchard JF, Kliewer E, et al. Cancer risk in patients with inflammatory bowel disease: a population-based study. *Cancer.* 2001;91:854–862.

3. Habermann J, Lenander C, Roblick UJ, et al. Ulcerative colitis and colorectal carcinoma: DNA-profile, laminin-5 gamma2 chain and cyclin A expression as early markers for risk assessment. *Scand J Gastroenterol.* 2001;36:751–758.

4. Terzic J, Grivennikov S, Karin E, et al. Inflammation and colon cancer. *Gastroenterology.* 2010;138:2101–2114.e2105.

5. Bartel DP. MicroRNAs: genomics, biogenesis, mechanism, and function. *Cell.* 2004;116:281–297.

6. He L, Hannon GJ. MicroRNAs: small RNAs with a big role in gene regulation. *Nat Rev Genet.* 2004;5:522–531.

7. O'Connell RM, Rao DS, Baltimore D. microRNA regulation of inflammatory responses. *Annu Rev Immunol.* 2012;30:295–312.

8. Esquela-Kerscher A, Slack FJ. Oncomirs—microRNAs with a role in cancer. *Nat Rev Cancer.* 2006;6:259–269.

9. Winter J, Jung S, Keller S, et al. Many roads to maturity: microRNA biogenesis pathways and their regulation. *Nat Cell Biol.* 2009;11:228–234.

10. Lu J, Getz G, Miska EA, et al. MicroRNA expression profiles classify human cancers. *Nature.* 2005;435:834–838.

11. Alvarez-Garcia I, Miska EA. MicroRNA functions in animal development and human disease. *Development.* 2005;132:4653–4662.

12. Cowland JB, Hother C, Gronbaek K. MicroRNAs and cancer. *APMIS.* 2007;115:1090–1106.

13. Taganov KD, Boldin MP, Chang KJ, et al. NF-kappaB-dependent induction of microRNA miR-146, an inhibitor targeted to signaling proteins of innate immune responses. *Proc Natl Acad Sci U S A.* 2006;103:12481–12486.

14. Chen R, Alvero AB, Silasi DA, et al. Regulation of IKKbeta by miR-199a affects NF-kappaB activity in ovarian cancer cells. *Oncogene.* 2008;27:4712–4723.

15. Lu Z, Li Y, Takwi A, et al. miR-301a as an NF-kappaB activator in pancreatic cancer cells. *EMBO J.* 2011;30:57–67.

16. Ludwig K, Fassan M, Mescoli C, et al. PDCD4/miR-21 dysregulation in inflammatory bowel disease-associated carcinogenesis. *Virchows Arch.* 2013;462:57–63.

17. Olaru AV, Yamanaka S, Vazquez C, et al. MicroRNA-224 negatively regulates p21 expression during late neoplastic progression in inflammatory bowel disease. *Inflamm Bowel Dis.* 2013;19:471–480.

18. Olaru AV, Cheng Y, Agarwal R, et al. Unique patterns of CpG island methylation in inflammatory bowel disease-associated colorectal cancers. *Inflamm Bowel Dis.* 2012;18:641–648.

19. Wu F, Zikusoka M, Trindade A, et al. MicroRNAs are differentially expressed in ulcerative colitis and alter expression of macrophage inflammatory peptide-2 alpha. *Gastroenterology.* 2008;135:1624–1635.e1624.

20. Gao J, Liu QG. The role of miR-26 in tumors and normal tissues (Review). *Oncol Lett.* 2011;2:1019–1023.

21. Palumbo T, Faucz FR, Azevedo M, et al. Functional screen analysis reveals miR-26b and miR-128 as central regulators of pituitary somatomammotrophic tumor growth through activation of the PTEN-AKT pathway. *Oncogene.* 2013;32:1651–1659.

22. Wu N, Zhao X, Liu M, et al. Role of microRNA-26b in glioma development and its mediated regulation on EphA2. *PLoS One.* 2011;6:e16264.

23. Gottardo F, Liu CG, Ferracin M, et al. Micro-RNA profiling in kidney and bladder cancers. *Urol Oncol.* 2007;25:387–392.

24. Liu XX, Li XJ, Zhang B, et al. MicroRNA-26b is underexpressed in human breast cancer and induces cell apoptosis by targeting SLC7A11. *FEBS Lett.* 2011;585:1363–1367.

25. Ji Y, He Y, Liu L, et al. MiRNA-26b regulates the expression of cyclooxygenase-2 in desferrioxamine-treated CNE cells. *FEBS Lett.* 2010;584:961–967.

26. Gramantieri L, Fornari F, Callegari E, et al. MicroRNA involvement in hepatocellular carcinoma. *J Cell Mol Med.* 2008;12:2189–2204.

27. Zhang C, Tong J, Huang G. Nicotinamide phosphoribosyl transferase (Nampt) is a target of microRNA-26b in colorectal cancer cells. *PLoS One.* 2013;8:e69963.

28. Zhang Z, Kim K, Li X, et al. MicroRNA-26b represses colon cancer cell proliferation by inhibiting lymphoid enhancer factor 1 expression. *Mol Cancer Ther.* 2014;13:1942–1951.

29. Podolsky DK. Inflammatory bowel disease. *N Engl J Med.* 2002;347:417–429.

30. Treem WR. Emerging concepts in celiac disease. *Curr Opin Pediatr.* 2004;16:552–559.

31. Oberhuber G, Granditsch G, Vogelsang H. The histopathology of coeliac disease: time for a standardized report scheme for pathologists. *Eur J Gastroenterol Hepatol.* 1999;11:1185–1194.

32. Neufert C, Becker C, Neurath MF. An inducible mouse model of colon carcinogenesis for the analysis of sporadic and inflammation-driven tumor progression. *Nat Protoc.* 2007;2:1998–2004.

33. Castro F, Dirks WG, Fahnrich S, et al. High-throughput SNP-based authentication of human cell lines. *Int J Cancer.* 2013;132:308–314.

34. Remmele W, Stegner HE. Recommendation for uniform definition of an immunoreactive score (IRS) for immunohistochemical estrogen receptor detection (ER-ICA) in breast cancer tissue [in German]. *Pathologe.* 1987;8:138–140.

35. Erhard F, Dolken L, Jaskiewicz L, et al. PARma: identification of microRNA target sites in AGO-PAR-CLIP data. *Genome Biol.* 2013;14:R79.

36. Beinder L, Faehrmann N, Wachtveitl R, et al. Detection of expressional changes induced by intrauterine growth restriction in the developing rat mammary gland via exploratory pathways analysis. *PLoS One.* 2014;9:e100504.

37. Hulsen T, de Vlieg J, Alkema W. BioVenn—a web application for the comparison and visualization of biological lists using area-proportional Venn diagrams. *BMC Genomics.* 2008;9:488.

38. Vlassov AV, Magdaleno S, Setterquist R, et al. Exosomes: current knowledge of their composition, biological functions, and diagnostic and therapeutic potentials. *Biochim Biophys Acta.* 2012;1820:940–948.

39. Yang HB, Liang W, Liu XX, et al. Detection of dynamic expression of microRNAs in vivo using a dual-fluorescence reporter system/miRNA Tracer in zebrafish [in Chinese]. *Yi Chuan.* 2012;34:1181–1192.

40. Chakilam S, Gandesiri M, Rau TT, et al. Death-associated protein kinase controls STAT3 activity in intestinal epithelial cells. *Am J Pathol.* 2013;182:1005–1020.

41. Zhang L, Nephew KP, Gallagher PJ. Regulation of death-associated protein kinase. Stabilization by HSP90 heterocomplexes. *J Biol Chem.* 2007;282:11795–11804.

42. Craig AL, Chrystal JA, Fraser JA, et al. The MDM2 ubiquitination signal in the DNA-binding domain of p53 forms a docking site for calcium calmodulin kinase superfamily members. *Mol Cell Biol.* 2007;27:3542–3555.

43. Bajbouj K, Poehlmann A, Kuester D, et al. Identification of phosphorylated p38 as a novel DAPK-interacting partner during TNFalpha-induced apoptosis in colorectal tumor cells. *Am J Pathol.* 2009;175:557–570.

44. Schetter AJ, Heegaard NH, Harris CC. Inflammation and cancer: interweaving microRNA, free radical, cytokine and p53 pathways. *Carcinogenesis.* 2010;31:37–49.

45. Leeper NJ, Raiesdana A, Kojima Y, et al. MicroRNA-26a is a novel regulator of vascular smooth muscle cell function. *J Cell Physiol.* 2011;226:1035–1043.

46. Zhao N, Wang R, Zhou L, et al. MicroRNA-26b suppresses the NF-kappaB signaling and enhances the chemosensitivity of hepatocellular carcinoma cells by targeting TAK1 and TAB3. *Mol Cancer.* 2014;13:35.

47. Benderska N, Schneider-Stock R. Transcription control of DAPK. *Apoptosis.* 2014;19:298–305.

48. Jin Y, Blue EK, Dixon S, et al. A death-associated protein kinase (DAPK)-interacting protein, DIP-1, is an E3 ubiquitin ligase that promotes tumor necrosis factor-induced apoptosis and regulates the cellular levels of DAPK. *J Biol Chem.* 2002;277:46980–46986.

49. Henshall DC, Araki T, Schindler CK, et al. Expression of death-associated protein kinase and recruitment to the tumor necrosis factor signaling pathway following brief seizures. *J Neurochem.* 2003;86:1260–1270.

50. Capoccia BJ, Jin RU, Kong YY, et al. The ubiquitin ligase Mindbomb 1 coordinates gastrointestinal secretory cell maturation. *J Clin Invest.* 2013;123:1475–1491.

51. Itoh M, Kim CH, Palardy G, et al. Mind bomb is a ubiquitin ligase that is essential for efficient activation of Notch signaling by Delta. *Dev Cell.* 2003;4:67–82.

52. Chen W, Casey Corliss D. Three modules of zebrafish Mind bomb work cooperatively to promote Delta ubiquitination and endocytosis. *Dev Biol.* 2004;267:361–373.

53. Barsi JC, Rajendra R, Wu JI, et al. Mind bomb1 is a ubiquitin ligase essential for mouse embryonic development and Notch signaling. *Mech Dev.* 2005;122:1106–1117.

54. Zhang L, Gallagher PJ. Mind bomb 1 regulation of cFLIP interactions. *Am J Physiol Cell Physiol.* 2009;297:C1275–C1283.

55. Coskun M, Bjerrum JT, Seidelin JB, et al. miR-20b, miR-98, miR-125b-1*, and let-7e* as new potential diagnostic biomarkers in ulcerative colitis. *World J Gastroenterol.* 2013;19:4289–4299.

56. Kloosterman WP, Plasterk RH. The diverse functions of microRNAs in animal development and disease. *Dev Cell.* 2006;11: 441–450.

57. Stefani G, Slack FJ. Small non-coding RNAs in animal development. *Nat Rev Mol Cell Biol.* 2008;9:219–230.

58. Chen X, Ba Y, Ma L, et al. Characterization of microRNAs in serum: a novel class of biomarkers for diagnosis of cancer and other diseases. *Cell Res.* 2008;18:997–1006.

59. Mitchell PS, Parkin RK, Kroh EM, et al. Circulating microRNAs as stable blood-based markers for cancer detection. *Proc Natl Acad Sci U S A.* 2008;105:10513–10518.

60. Bai J, Li Y, Shao T, et al. Integrating analysis reveals microRNA-mediated pathway crosstalk among Crohn's disease, ulcerative colitis and colorectal cancer. *Mol BioSyst.* 2014;10:2317–2328.